In humanoid robots, as in humans, bipedal standing should come before bipedal walking: implementing the Functional Reach Test

Vishwanathan Mohan, Jacopo Zenzeri, Giorgio Metta and Pietro Morasso

Abstract This chapter describes a computational architecture for coordinating the degrees of freedom of the humanoid robot iCUB during bipedal standing, with particular reference to the Whole Body Reaching and the Functional Reach Test.

1 Introduction

In humans the ability to stand up on two legs is a necessary prerequisite for bipedal walking. Moreover, there is ample neurophysiological evidence that standing and walking are rather independent control mechanisms. Therefore, we suggest that also humanoid robots should be trained first to master the unstable standing posture and then learn to walk.

We shall address such issue in relation with the humanoid robot iCub [1], which has the size of a three years old child (height is 105 cm and weight is 14.2 kg) and has 53 degrees of freedom (DoF): 7 DoFs for each arm, 9 for each hand, 6 for the head, 3 for the trunk and spine and 6 for each leg. iCub is still unable to stand or walk, but only to crawl, as baby toddlers of the same age. Therefore, the goal of this paper is to carry out a preliminary study of the computational processes that may allow iCub to achieve the sensorimotor competence that is necessary for bipedal

Vishwanathan Mohan
RBCS Dept, Italian Institute of Technology, Genova, Italy e-mail: vishwanathan.mohan@iit.it

Jacopo Zenzeri
RBCS Dept, Italian Institute of Technology, Genova, Italy e-mail: jacopo.zenzeri@iit.it

Giorgio Metta
RBCS Dept, Italian Institute of Technology, Genova, Italy and DIST, University of Genova, Genova, Italy e-mail: giorgio.metta@iit.it

Pietro Morasso
RBCS Dept, Italian Institute of Technology, Genova, Italy and DIST, University of Genova, Genova, Italy e-mail: pietro.morasso@unige.it

standing. The study builds upon what has already been achieved in the bimanual coordination of iCub's movements [2], using a biomimetic, force-field based computational model. The model has been evaluated and validated both in a simulated environment and in real movements. On the contrary, the present study is limited to the simulation stage for 'developmental constraints', because the sensorimotor system of iCub has not matured enough to achieve the features that are necessary for standing (postural control system) and walking (bipedal locomotion system).

As a matter of fact, the postural control system must face two main problems: P1) stabilize the inverted pendulum that characterizes the bipedal standing posture either during quiet standing or when compensating the postural perturbations induced by movements of the upper part of the body; P2) coordinate the redundant set of DoFs of the lower and upper parts of the body in whole body gestures. The focus of this paper is on P2.

The easiest way to solve P1 would be to use a 'stiffness strategy', in particular at the ankle joint. However, this is not what humans do, because the ankle stiffness is dominated by the elasticity of the Achilles tendon and the corresponding stiffness is consistently smaller than the toppling torque due to gravity [3, 4]. Different studies have shown that the ankle torque which is missing from the intrinsic properties of the soft ankle tendons is likely to be supplemented by an active control process [5, 6]: this process can be characterized as an intermittent control mechanism that generates frequent, ballistic bias impulses by soleus and gastrocnemius. It was also shown [7] that this discrete-time feedback controller is much more robust and thus more plausible that an alternative continuous time control mechanism [8] if one considers the large transmission delays in the feedback loop and the intrinsic instability of the bodily inverted pendulum. There is a functional merit to the low-stiffness solution of the postural stabilization mechanism because a rather compliant ankle joint avoids high impact forces with the ground and more easily adapts to uneven surfaces. In other words, a low-stiffness postural controller is more robust and is capable of guaranteeing stability in a much wider range of situations than a stiff controller.

P2 implies a quite different computational problem because functional movements during bipedal standing recruit, in principle, all the DoFs of the global kinematic chain, with a high degree of redundancy, whereas P1 can be considered a 1 DoF or 2 DoFs 'ankle strategy'. As already mentioned, we plan to address this problem by using a biomimetic, force-field based computational model, which takes inspiration from the Passive Motion Paradigm (PMP [9]), extended to include terminal attractor properties [10]. We already used this approach for the coordination of bimanual movements of the humanoid robot iCub [2] and for modeling whole body reaching (WBR) movements in humans [11]. Here we investigate the feasibility of applying this model to the coordination of WBR movements in iCub, with particular emphasis on a specific form of WBR, the Functional Reach Test (FRT), which has been invented as a dynamic clinical measure of balance [12]. FRT measures the distance between the length of the arm and a maximal forward reach in the standing position, while maintaining a fixed base of support. FRT has been tested for both validity and reliability and is used in patients with diagnoses as different as stroke,

Parkinson, vestibular hypofunction, multiple sclerosis and hip fractures. FRT has also been associated with an increased risk of fall and frailty in elderly people who are unable to reach more than 15 cm.

Since the current state of the iCub's competence for the standing posture has some 'pathological' aspects, the improvements coming from better design and better control could be appropriately evaluated with a FRT similar to the one used with humans.

2 FRT network for iCub

The network architecture which has been developed for allowing iCub to face the Functional Reaching Test is an extension of the architecture developed for modeling whole body reaching movements in humans [11]. The architecture is composed of four parts: 1) Task sub-network, 2) Focal sub-network, 3) Postural sub-network, 4) Temporal coordination unit (see Fig. 1).

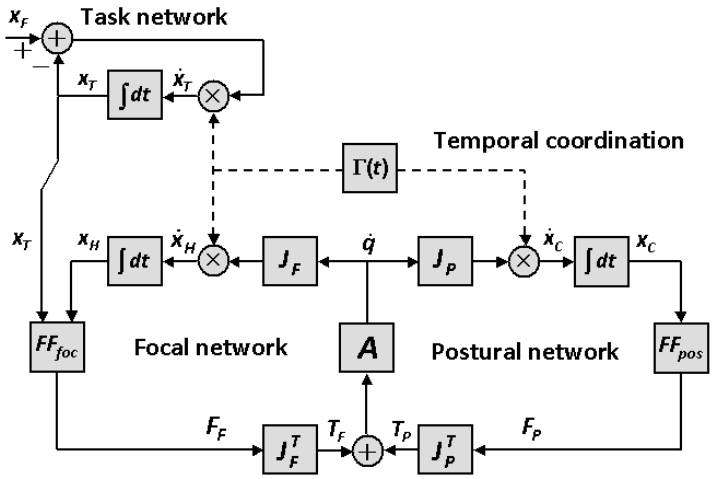

Fig. 1 FRT network for iCub. $\mathbf{x}_F$, $\mathbf{x}_T$, $\mathbf{x}_H$, $\mathbf{x}_C$, $\mathbf{q}$: vectors of the final and current target position, position of the CoM, and the joint configuration, respectively; $\mathbf{J}_F$, $\mathbf{J}_P$: Jacobian matrices of the focal and postural sub-networks, respectively; $\mathbf{FF}_{foc}$, $\mathbf{FF}_{pos}$: force field generators of the focal and postural sub-networks, respectively; $\mathbf{A}$: admittance matrix; Γ: temporal coordination function.

The three networks are stable dynamical systems with terminal-attractor characteristics, which is provided by the temporal coordination unit. This unit generates a time-varying gain which is transmitted to the three sub-networks and allows them to reach final equilibrium at the same time:

$$\begin{cases} \Gamma(t) = \frac{\dot{\xi}}{(1-\xi)} \\ \xi(t) = 6\left(\frac{t-t_0}{\tau}\right)^5 - 15\left(\frac{t-t_0}{\tau}\right)^4 + 10\left(\frac{t-t_0}{\tau}\right)^3 \end{cases} \quad (1)$$

Here t_0 is the initiation time and τ is the duration of the coordinated forward reaching movement; $\xi(t)$ is a minimum jerk time base generator, but any smooth function with similar temporal features would yield the same results in terms of temporal coordination of the three sub-networks.

The task sub-network generates a moving target $\mathbf{x}_T$ in 3D which attracts both hands of iCub (represented by the time-varying vector $\mathbf{x}_H$) with a suitable force field, generated by the focal sub-network. $\mathbf{x}_T$ evolves from the initial position of the hands, which are supposed to be jointed, to a final position $\mathbf{x}_F$. This is related to the most common form of FRT, i.e. the bimanual test. We might also implement in the same framework a unimanual paradigm in which one hand is attracted by a forward moving target and the other is either fixed or is used as a further balancing tool. In WBR experiments $\mathbf{x}_F$ may be situated beyond arm's length but should be placed inside the reachable workspace, defined as the set of points that can be reached by keeping the projection on the ground of the center of mass (CoM) within the support base of the standing robot. Obviously, the support base is a function of the position of the feet and in FRT they are supposed to be parallel and symmetric with respect to the body. In FRT experiments we also positioned $\mathbf{x}_F$ just outside the reachable workspace, in the anterior-posterior direction.

The focal sub-network generates an attractive force field of elastic type which is applied to both hands, implementing the focal part of the task whose goal is to allow the hand to reach the target: $\mathbf{F}_F = \mathbf{K}_F(\mathbf{x}_T - \mathbf{x}_H)$. $\mathbf{K}_F$ is a 3x3 matrix and for simplicity we assumed that it is diagonal. Moreover, in the logic of FRT the force field should be directed in anterior-posterior direction and thus only one component of the matrix is non-zero. The field $\mathbf{F}_F$ is mapped from the extrinsic space to the joint space ($\mathbf{T}_F$) by the following transformation, where $\mathbf{J}_F$ is the Jacobian matrix of the overal kinematic chain (from feet to hands): $\mathbf{T}_F = \mathbf{J}_F^T \mathbf{F}_F$. The admittance matrix $\mathbf{A}$ transforms this torque field into a movement vector $\dot{\mathbf{q}}$ of the kinematic chain, which is mapped to the extrinsic space by the same Jacobian matrix, generating the trajectory of the hand $\mathbf{x}_H$ and thus closing the loop. This dynamical mechanism allows the hand to reach $\mathbf{x}_F$ at the same time in which $\mathbf{x}_T$ reaches $\mathbf{x}_F$, but there is no guarantee that the CoM remains withing the support base in the process. Thus, if only driven by this mechanism, iCub would reach the target but fall forward immediately after. The postural sub-network is intended to prevent such unfortunate event.

The postural sub-network modifies the torque field $\mathbf{T}_F$, generated by the focal sub-network, by adding a component $\mathbf{T}_P$ that takes into account the position of the CoM on the support base ($\mathbf{T}_{TOT} = \mathbf{T}_F + \mathbf{T}_P$). In the vein of the so called 'hip strategy', which characterizes human postural movements, the postural force field is applied to the hip joint and pulls it backward as function of the distance of the CoM from the forward limit of the support base. The activation of the field is meant to induce the following effects: 1) a smaller forward shift of the CoM; 2) a backward shift of the hip; 3) a forward tilt of the trunk associated with the lowering of the CoM. It is worth remarking that this complex control pattern is not explicitly rep-

resented but is implicitly coded by the dynamics of the network. The motion of the CoM $\mathbf{x}_C$ is derived from the motion of the whole kinematic chain using a different Jacobian matrix $\mathbf{J}_F$ that only takes into account the ankle and knee joints. The force field applied to the hip was implemented by a non-linear function that diverges to very high values when $\mathbf{x}_C$ approaches the forward limit of the support base $\mathbf{x}_{MAX}$.

In summary, the integrated dynamics of the interacting sub-networks is characterized by the following equations, which achieve a balance between the forward pull applied to the hand and the backward pull applied to the hip:

$$\begin{cases} \dot{\mathbf{x}_T} = \Gamma(t)\,(\mathbf{x}_F - \mathbf{x}_T) \\ \dot{\mathbf{x}_H} = \Gamma(t)\mathbf{J}_F\mathbf{A}\mathbf{T}_{TOT} \\ \dot{\mathbf{x}_C} = \Gamma(t)\mathbf{J}_P\mathbf{A}\mathbf{T}_{TOT} \\ \mathbf{T}_{TOT} = \mathbf{T}_F + \mathbf{T}_P \\ \mathbf{T}_F = \mathbf{J}_F^T\mathbf{K}_F\,(\mathbf{x}_F - \mathbf{x}_T) \\ \mathbf{T}_P = \mathbf{J}_P^T\mathbf{K}_P\,\frac{\mathbf{x}_C}{|\mathbf{x}_{MAX} - \mathbf{x}_C| + \varepsilon}\,(\mathbf{x}_T - \mathbf{x}_H) \end{cases} \tag{2}$$

3 Simulation experiments with FRT network

The computational architecture described in the previous section was tested by using the iCub simulator. The robometric parameters of iCub (length, mass) are summarized here: leg (0.213 m, 0.95 kg); thigh (0.224 m, 1.5 kg); trunk (0.127 m, 4 kg); humerus (0.152 m, 1.15 kg); forearm + hand (0.137 m, 0.5 kg). The head weight is 2 kg.

As suggested by the FRT protocol, the initial posture of the test is characterized the following set of joint angles (ordered from the ankle joint to the elbow joint): 85°, 92°, 85°, 330°, 0°. These are absolute values, referred to a horizontal line. With this posture the initial position of the hand reaches a distance of 29.05 cm beyond the vertical line and the CoM is shifted forward 3.87 cm with respect to the ankle joint. The final position of the target was set 5 cm beyond the maximum reachable forward distance and the limit for the CoM displacement ($\mathbf{x}_{MAX}$) was set equal to 13 cm, considering that the length of iCub's foot is 15 cm.

The basic parameters of the FRT control network are 1) the gain of the focal field **KF**, 2) the gain of the local field **KP**, 3) and the admittance matrix of the whole kinematic chain **A**. The latter is a 5x5 matrix but we assumed for simplicity that it is diagonal and thus we only have to choose 5 parameters. The results of the simulations make us confident that the choice of these parameters is not critical. The simulations reported in the following were obtained with the following list of values: **KF**=700N/m; **KP**=2N; **A1**(ankle)=0.02rad/Nms; **A2**(knee)=0.01rad/Nms; **A3**(hip)=0.3rad/Nms; **A4**(shoulder)=0.1rad/Nms; **A5**(elbow)=0.07rad/Nms. In particular, as discussed in [11], the choice of the **A** parameters allows iCub to choose among equivalent solutions of the planned movement, as a consequence of the redundancy of the kinematic chain.

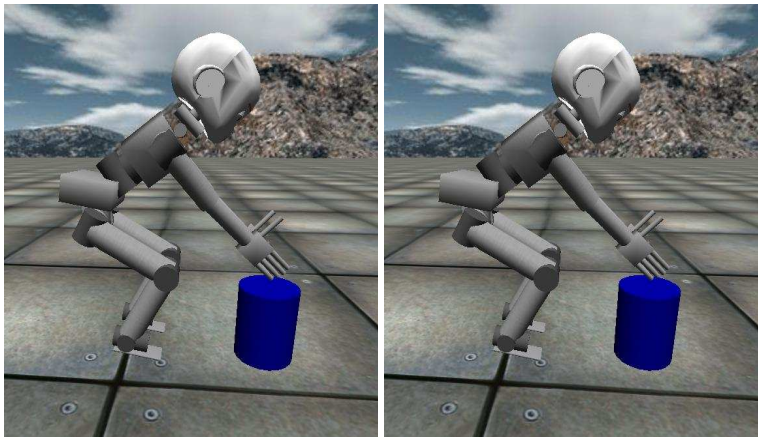

Fig. 2 Initial and final poses of iCub in the Functional Reaching Test.

Figure 2 shows the initial and final posture of the FRT, which allowed iCub to reach forward at a distance of 47.39cm, with an increase of 18.35cm with respect to the initial posture. Incidentally, this value is greater than the threshold of 15cm which is considered clinically relevant in relation with the risk of falling.

Figure 3 shows the evolution of the different relevant variables. Panel A displays the intensities of the focal and postural force fields, respectively. Panel B shows the joint rotations patterns from the initial to the final posture, reached at the time of termination of the Γ function. Please note that some angles evolve monotonously from initial to termination time whereas other do not. In particular, the elbow joint angle remains equal to 0 throughout the whole movement for two reasons: 1) it was set to 0 initially in agreement with the FRT protocol and 2) it remained 0 because both force fields were directed horizontally (the focal field forward and the postural field backward, respectively). Panel C plots the forward displacements of the hand and the CoM, respectively. The curves evolve monotonously, as should do, to the final shift values that must be compared with the final position of the target and the maximum admitted forward shift of the CoM, respectively. It turns out that the hand stops 5 cm before the target, because the latter is outside the workspace of the robot; the CoM stops just 6 mm before the fixed limit. Finally, panel D displays the speed profiles of the hand and the CoM respectively: they appear to be bell-shaped and synchronized, in agreement with the basic findings of the research in WBR [13, 14, 15]. Panels A, B, C also display the time course of the Γ function, emphasizing its role in the ordered coordination and synchronization of so many different variables.

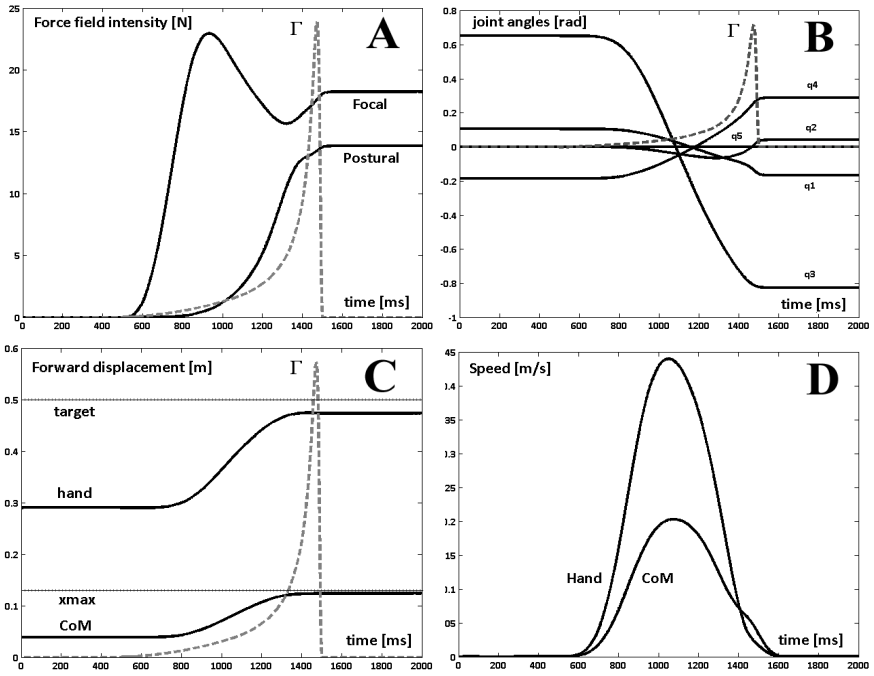

Fig. 3 *Panel A*: time course of the forces generated by the focal and the postural sub-networks, respectively. *Panel B*: Time course of the joint rotation angles, after subtracting the mean value: q1(ankle)=1.38 rad; q2(knee)=1.60 rad; q3(hip)=0.83 rad; q4(shoulder)=5.95 rad; q5(elbow)=0 rad. The angular values are absolute, referred to the horizontal line. *Panel C*: forward shift of the hand (Functional Reach), related to the forward position of the target (5 cm beyond the workspace) and forward shift of the CoM, related to the maximum stable position on the support base. *Panel D*: velocity profiles of the hand and the CoM. Panels A, B, C also display the time course of the Γ function.

4 Discussion

The proposed coordination model is not a controller of the standing posture but a mechanism of synergy formation, which allows the redundant DoFs to be coordinated in a principled way during manipulation tasks that may affect the stability of the standing posture. The proposed computational layer is 'cognitively penetrable' and is somehow uncoupled from the lower-level control mechanisms that maintains the dynamic stability of the bipedal standing posture.

Acknowledgements This work was supported by the RBCS Department of the Italian Institute of Technology and FP7 EU Projects Humour and iTalk.

References

1. Natale, L., Orabona, F., Metta, G., Sandini, G. (2007) Sensorimotor coordination in a 'baby' robot: learning about objects through grasping. Prog Brain Res, 164,403-24
2. Mohan V, Morasso P, Metta G, Sandini G (2009) A biomimetic, force-field based computational model for motion planning and bimanual coordination in humanoid robots. Auton Robots 27:291-307
3. Loram ID, Lakie M (2002) Direct measurement of human ankle stiffness during quiet standing: the intrinsic mechanical stiffness is insufficient for stability. J Physiol 545:1041-1053
4. Casadio M, Morasso P, Sanguineti V (2005) Direct measurement of ankle stiffness during quiet standing: implications for control modelling and clinical application. Gait & Posture, 21:410-424
5. Loram ID, Maganaris CN, Lakie M (2005). Human postural sway results from frequent, ballistic bias impulses by soleus and gastrocnemius. J Physiol 564(1):295-311
6. Bottaro A, Yasutake Y et al (2008) Bounded stability of the quiet standing posture: an intermittent control model. Hum Mov Sci 27:473-95
7. Asai Y, Tasaka Y et al (2009) Postural stabilization of quiet standing by means of PD feedback: and intermittent, switching control strategy is more robust than the linear, continuous-time strategy and better captures the spectral properties of human sway. PLoS ONE, 4:e6169
8. Maurer C, Peterka R (2005) A new interpretation of spontaneous sway measures based on a simple model of human postural control. J Neurophysiol 93:189-200
9. Mussa Ivaldi FA, Morasso P, Zaccaria R (1988) Kinematic Networks. a distributed model for representing and regularizing motor redundancy. Biol Cybern 60:1-16
10. Zak M (1988) Terminal attractors for addressable memory in neural networks. Phys. Lett. A 133:218-222
11. Morasso P, Casadio M, Mohan V, Zenzeri J (2009) A neural mechanism of synergy formation for whole body reaching. Biol Cybern 102:291-307
12. Duncan PW, Weiner DK, Chandler J, Studenski S (1990) Functional reach: a new clinical measure of balance. J Gerontol 45:M192-M197
13. Stapley PJ, Cheron G, Grishin A (1999) Does the coordination between posture and movement during human whole-body reaching ensure center of mass stabilization? Exp Brain Res 129:134-46
14. Pozzo T, Stapley PJ, Papaxanthis C (2002) Coordination between equilibrium and hand trajectories during whole body pointing movements. Exp Brain Res, 144:343-350
15. Kaminski TR (2007) The coupling between upper and lower extremity synergies during whole body reaching. Gait & Posture 26:256-262